

# Arrangement of the Heads of Myosin in Relaxed Thick Filaments from Tarantula Muscle

R. A. Crowther, Raúl Padrón† and Roger Craig‡

MRC Laboratory of Molecular Biology  
Hills Road, Cambridge CB2 2QH, U.K.

(Received 6 November 1984, and in revised form 28 March 1985)

Thick filaments from leg muscle of tarantula, maintained under relaxing conditions (Mg-ATP and EGTA), were negatively stained and photographed with minimal electron dose. Particles were selected for three-dimensional image reconstruction by general visual appearance and by the strength and symmetry of their optical diffraction patterns, the best of which extend to spacings of  $1/5 \text{ nm}^{-1}$ . The helical symmetry is such that, on a given layer-line, Bessel function contributions of different orders start to overlap at fairly low resolution and must therefore be separated computationally by combining data from different views. Independent reconstructions agree well and show more detail than previous reconstructions of thick filaments from *Limulus* and scallop. The strongest feature is a set of four long-pitch right-handed helical ridges (pitch  $4 \times 43.5 \text{ nm}$ ) formed by the elongated myosin heads. The long-pitch helices are modulated to give ridges with an axial spacing of  $14.5 \text{ nm}$ , lying in planes roughly normal to the filament axis and running circumferentially. We suggest that the latter may be formed by the stacking of a subfragment 1 (S1) head from one myosin molecule on an S1 from an axially neighbouring molecule. Internal features in the map indicate an approximate local twofold axis relating the putative heads within a molecule. The heads appear to point in opposite directions along the filament axis and are located very close to the filament backbone. Thus, for the first time, the two heads of the myosin molecule appear to have been visualized in a native thick filament under relaxing conditions.

## 1. Introduction

The thick filaments of striated muscle are bipolar structures bearing myosin crossbridges, which are responsible for filament sliding during muscular contraction (Huxley, 1957, 1963, 1969). They are formed by polymerization of myosin molecules whose tails lie in the filament backbone and whose two heads (which together we term a crossbridge) lie at the surface where they are free to interact with actin (Huxley, 1963). X-ray diffraction shows that the crossbridges in relaxed muscle are helically arranged but does not reveal the precise symmetry or crossbridge shape (Huxley & Brown, 1967; Wray *et al.*, 1975). Methods have been developed recently for the preservation of the three-dimensional arrangement of crossbridges in negatively stained

thick filaments (Kensler & Levine, 1982a). It has thus been possible to determine the rotational symmetry, helix handedness and low resolution crossbridge shape in several muscles (Stewart *et al.*, 1981; Kensler & Levine, 1982b; Vibert & Craig, 1983; Kensler & Stewart, 1983). The crossbridges appear as elongated units that are tilted and slewed with respect to the filament axis, but the two heads within a crossbridge have not been resolved.

We report here a study by electron microscopy and image analysis of tarantula muscle thick filaments, which are particularly suitable for a detailed structural study, since X-ray diffraction shows that these filaments have highly ordered crossbridge arrays (Wray, 1982). Filaments in the relaxed state have been negatively stained with uranyl acetate and low electron dose micrographs recorded to maximize resolution and image fidelity (Williams & Fisher, 1970; Unwin, 1974). Image analysis has been carried out by computer programs that separate overlapping Bessel functions on the same layer-line, thus further enhancing detail. Three-dimensional reconstructions reveal a four-stranded, right-handed helical arrangement of crossbridges, each resolvable into

† Present address: Laboratorio de Biofísica del Músculo, Centro de Biofísica y Bioquímica, Instituto Venezolano de Investigaciones Científicas (IVIC), Apdo 1827 Caracas 1010A, Venezuela.

‡ Present address: Department of Anatomy, University of Massachusetts Medical School, 55 Lake Avenue North, Worcester, MA 01605, U.S.A.

two myosin heads, which apparently overlap between one axial level and the next. These reconstructions provide the basis for a study of the structural changes that occur in these filaments in different physiological states (Craig *et al.*, 1985).

Preliminary reports of this work have appeared elsewhere (Craig & Padrón, 1982; Padrón *et al.*, 1984).

## 2. Materials and Methods

### (a) Preparation of filaments

Mexican red-knee tarantulas (*Brachypelma sp.*, sex unknown) were cooled at 4°C for 1 h and their legs removed and dissected at room temperature. Muscles of the femur and tibia were exposed by cutting away longitudinally about one-third to one-half of the exoskeleton of each segment. The segments were then transferred immediately to vials containing 20 ml of ice-cold demembrating solution, consisting of fresh relaxing medium (100 mM-NaCl, 8 mM-MgCl<sub>2</sub>, 5 mM-EGTA, 10 mM-sodium phosphate, 3 mM-NaN<sub>3</sub>, 5 mM-ATP, 1 mM-dithiothreitol (pH 7.0)) containing 0.1% (w/v) saponin (Vibert & Craig, 1983; Padrón & Huxley, 1984). The vials were agitated by rotation at about 60 revs/min for 3 to 4 h at 4°C and the muscles then transferred to fresh relaxing solution (without saponin) and left in this overnight or up to 3 days at 0°C, with a change to fresh relaxing medium each day.

Filaments were prepared from these skinned muscles as described by Vibert & Craig (1983), except that just after homogenization a "cocktail" of enzyme inhibitors consisting of 20 µl of 100 mM-phenylmethylsulphonyl fluoride in isopropanol and 200 µl of a freshly thawed solution of 1 mg leupeptin/l (Sigma, L-2884), 1 mg pepstatin A/l (Sigma, P-4265), 10 mg alpha-N-benzoyl-L-arginine ethyl ester hydrochloride/l (Sigma, B-4500), 10 mg *p*-toluenesulphonyl-L-arginine methyl ester hydrochloride/l (Sigma, T-4626), and 10 mg trypsin inhibitor/l from chicken egg-white type II-0 (Sigma, T-9253), were added in order to reduce proteolysis (following a suggestion of J. Kendrick-Jones, personal communication).

### (b) Electron microscopy

Negative staining of filaments, using 1% (w/v) uranyl acetate on holey carbon films, and subsequent stabilization of the grids by a light coating of carbon were carried out essentially as described by Vibert & Craig (1982, 1983). The grid was rinsed with a relaxing solution of 0.1 M-sodium acetate, 2 mM-magnesium acetate, 0.2 mM-EGTA, 1 mM-ATP, 2 mM-imidazole, 3 mM-NaN<sub>3</sub> (pH 7.0) immediately before staining. This replaces the rinse with a simple 0.1 M-ammonium acetate solution used previously (Kensler & Levine, 1982a; Vibert & Craig, 1983) and instead maintains the filaments in a relaxing medium until the instant of staining. An acetate-based rinse rather than one based on chloride was essential for the preservation of helical order in the negatively stained filaments. Grids were prepared soon after isolation of filaments (usually within 2 to 3 h), since the crossbridge order in the filaments deteriorated with time.

Grids were examined in a Philips EM400 electron microscope operated at 80 kV with a 20 µm objective aperture, a 200 µm C2 aperture and an anti-contamination cold finger. Filaments suspended in stain

over holes in the carbon appeared to be better ordered than those on the carbon itself, as reported by Vibert & Craig (1983). The best contrast and order were observed in medium thickness sheets of stain. Only filaments lying in unbroken films of stain over holes were used for image processing. An initial study was made with normal high dose pictures, which allowed us to determine adequate conditions for the best preservation of helical order. Photographing the filaments for 3-dimensional reconstruction was performed on previously unexplored grids using the minimal electron dose technique (Unwin & Henderson, 1975) with the aid of the low dose kit on the EM400 microscope. An estimated electron dose of 10 to 15 e/Å<sup>2</sup> was used, with a 1 µm spot size and a high beam current (approx. 40 µA) to improve beam coherence. Filaments were photographed at 25,000× nominal magnification, and tropomyosin paracrystals (39.5 nm repeat) were photographed under the same conditions during each photographic session at the same magnification to calibrate the electron-optical magnification.

For determination of the handedness of the dominant helical family, filaments were unidirectionally shadowed with Pt as described by Vibert & Craig (1983).

### (c) Image analysis and three-dimensional reconstruction

Optical diffraction patterns of selected filaments lying in unbroken sheets of stain over holes were recorded with the surveying diffractometer (DeRosier & Klug, 1972). Particles were selected for computer processing by general visual appearance and by optical diffraction. Those areas giving the strongest and most symmetrical diffraction patterns were digitized with a computer-controlled film scanner (Arndt *et al.*, 1969), on a raster corresponding to 8.4 Å sampling of the original image. All images were oriented in the same way from bare-zone to tip before densitometry.

Standard computer programs for analysing helical particles (DeRosier & Moore, 1970; Amos, 1975), adapted for the VAX 11-780, were used. An additional program was written to allow separation of overlapping Bessel function contributions on a given layer-line by combining data from particles in different orientations. In order to do this, the relative azimuthal orientations and origins of the different particles were first found by comparing those parts of the layer-lines nearest the meridian, where only a single Bessel function contributes.

On each layer-plane the transform value  $F(R, \Phi)$  can be expressed as a sum over the allowed Bessel function contributions  $G_n(R)$  on that layer, namely:

$$F(R, \Phi) = \sum_n G_n(R) i^n e^{in\Phi}$$

Two-dimensional transforms of the various particles in different orientations give values  $F(R, \Phi_j)$  of the 3-dimensional transform at a set of angular positions  $\Phi_j$ , for each radius  $R$ , on a given layer-plane, so that:

$$F(R, \Phi_j) = \sum_n G_n(R) i^n e^{in\Phi_j} \quad (1)$$

For an arbitrary set of views these equations, split into real and imaginary parts, can then be solved at each radius  $R$  by least squares to give the separate Bessel contributions  $G_n(R)$  on each layer-plane (Crowther *et al.*, 1970; Amos, 1976). The least-squares residuals, considered particle by particle or layer-plane by layer-plane, may then be used to assess the quality of the data and if necessary eliminate any particles which agree poorly with the others.

### 3. Results

Thick filaments, isolated by the method described, appeared well-preserved and intact, with an approximate length of 4 to 5  $\mu\text{m}$  and a centrally located bare zone of length about 210 nm (Fig. 1(a)). The filaments have a diameter of 20 nm

in the bare zone and an overall diameter of 32 nm in the crossbridge region, measured to the outermost boundary of the heads.

Filaments shadowed unidirectionally with platinum (Fig. 1(b)) show prominent long-pitch helices which are right-handed, as previously shown by Levine *et al.* (1983). The correctness of this

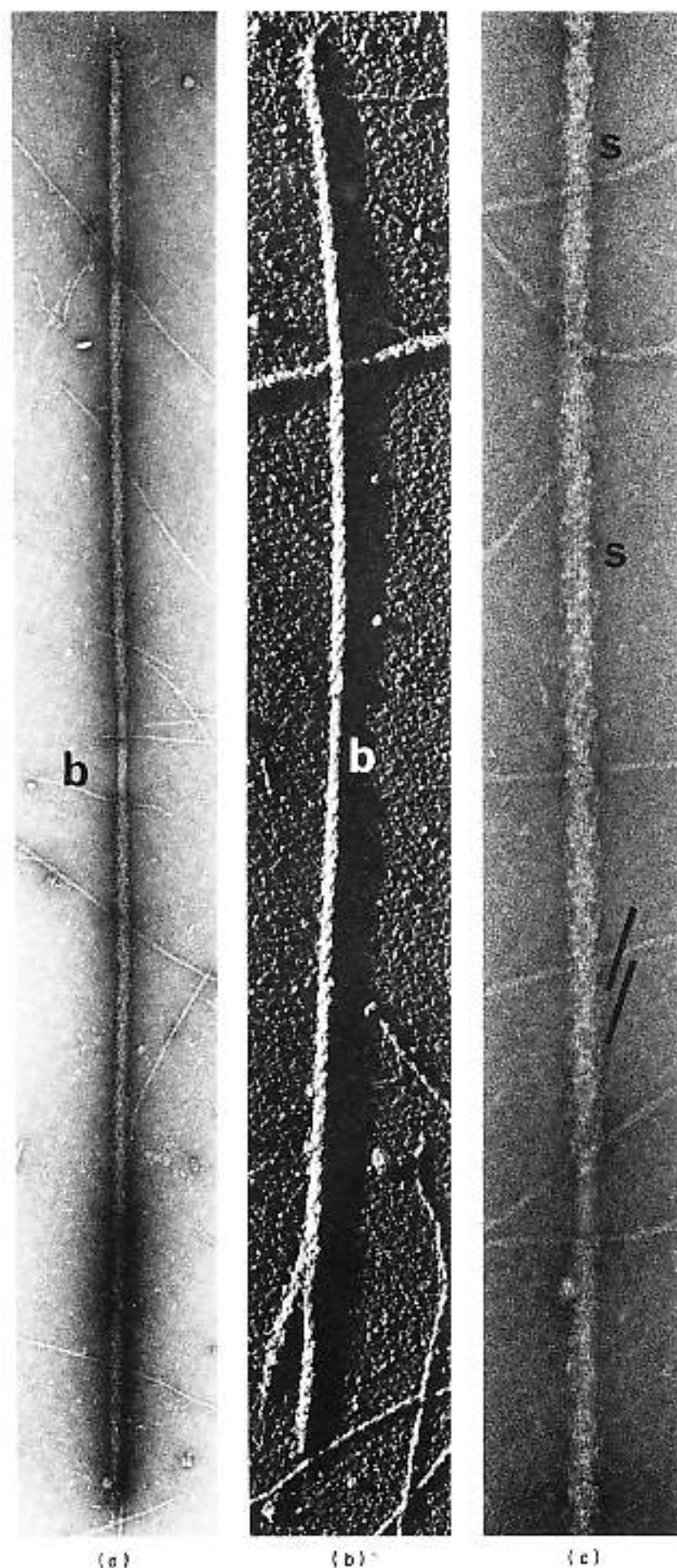


**Figure 1.** Electron micrographs of tarantula thick filaments. (a) Negatively stained whole filament showing the central bare zone. b. (b) Shadowed filament, showing the central bare zone with prominent sets of right-handed long-pitch helices of crossbridges on either side of it. The photographic contrast of the micrograph has been reversed before printing, so deposited metal appears white. (c) Higher magnification view of a negatively stained filament that, when viewed obliquely, shows clearly the long-pitch helices of crossbridges (bars). Prominent longitudinal striping (s) arising from the backbone is also visible in various parts of the filament. Actin thin filaments are visible in the backgrounds. Approximate magnifications: (a) 55,000 $\times$ ; (b) 48,000 $\times$ ; (c) 146,000 $\times$ .

determination is confirmed by simultaneous observation of thin filaments, which also appear right-handed (Depue & Rice, 1965). The handedness of the helix is the same on both sides of the bare zone. In some favourable alignments, a 14.5 nm transverse banding is also seen.

Negatively stained filaments (Fig. 1(a) and (c), and Fig. 2) display the same prominent helical tracks that are seen in the shadowed pictures and also show transverse banding with a spacing of 14.5 nm, corresponding to the repeating levels of crossbridges. In some regions of the filaments (Fig. 1(c)), there appear to be longitudinal striations with an approximate side-to-side spacing of 4 nm, apparently consistent with Wray's (1979, 1982) subfilament model of the thick filament backbone. However, we have not been able to make a detailed interpretation of these features in terms of the packing of the rod parts of the myosin molecules. Particles showing such longitudinal striping appeared to have less well-ordered crossbridges and were not used in the reconstruction. A montage of some of the filaments used for the three-dimensional reconstruction is shown in Figure 2.

Computed transforms from selected regions of two particles are shown in Figure 3. The patterns display a clear series of layer-lines indexing on an approximate 43.5 nm repeat. For standardization, all data were scaled to the 43.5 nm repeat indicated by X-ray measurements (Wray, 1982). The meridional reflections on the third and sixth layer-lines corresponding to axial spacings of 14.5 nm and 7.25 nm are particularly clear, as are the first and fourth layer-lines, in agreement with Levine *et al.* (1983). In some computed transforms, the seventh, eighth and ninth (meridional) layer-lines are also seen, though they are always weak. The relative intensities of the layer-lines appear to agree quite well with those seen in X-ray diffraction patterns of relaxed tarantula muscle (kindly provided by J. S. Wray, personal communication). This suggests that

the helical order has been preserved and that the filaments retain key features of their native relaxed structure after being stained.

Levine *et al.* (1983) established that the crossbridges on the tarantula thick filament have fourfold rotational symmetry and that there is a rotation of 30° between successive 14.5 nm levels of crossbridges, so that they lie on a set of four-start long-pitch helices, each with 12 units per turn. Our data agree with this conclusion. This combination of symmetry operations means that the structure repeats after  $3 \times 14.5$  nm (i.e. 43.5 nm), but that this axial period contains only six independent views of the asymmetric unit. The helical indexing scheme, shown in Figure 4, thus indicates an overlap of Bessel function contributions even at quite low resolution, so that a three-dimensional reconstruction cannot be made from a single view of the filament. It is therefore necessary to combine data from a number of different particles lying in different orientations to separate out the various Bessel function contributions on each layer-line, as described in Materials and Methods, section (c).

The relative orientations and axial displacements must first be found and this can be done by comparing those parts of the layer-lines closest to the meridian where there is only a single Bessel function contributing. An average of the two sides of the strongest and most symmetrical transform was taken as reference and all the other particles were fitted to this. Independent reconstructions made from two sets, each of five particles, agreed well. The best four particles from each set, judged by the least-squares residuals when solving the equations for the  $G_n$  term (Materials and Methods, section (c)), were then combined to make the reconstruction to be described here. The separated Bessel function contributions to the various layer-lines are shown in Figure 5 and data on the fitting of the particles are summarized in Table 1. For the reconstruction, data were included out to the ninth

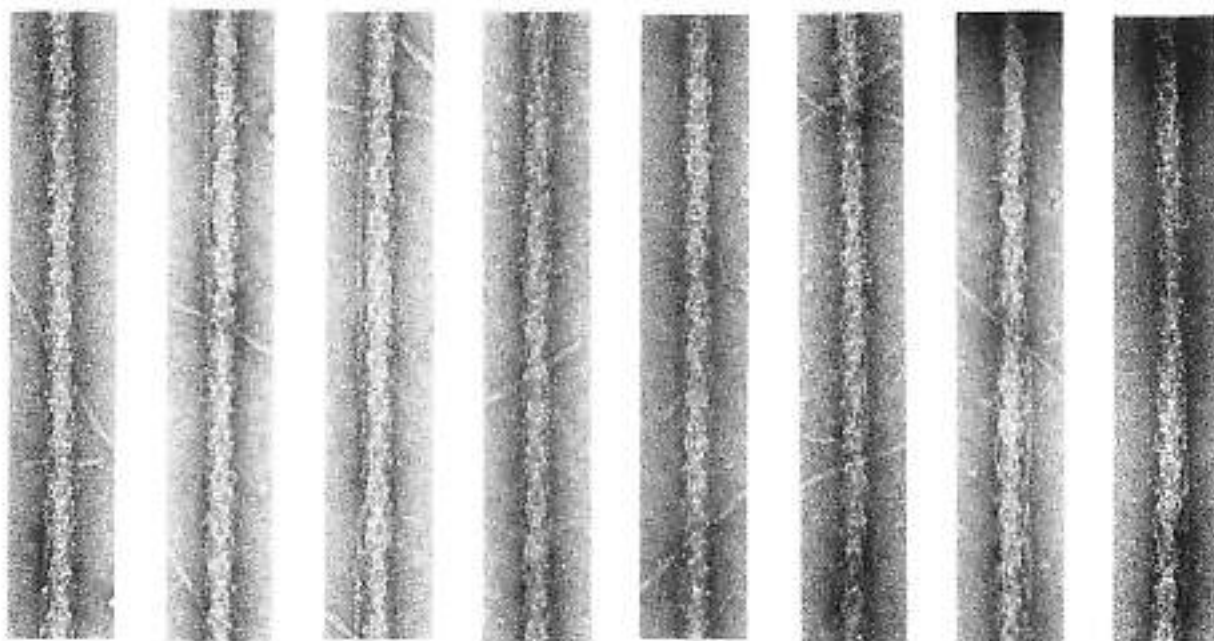


**Figure 2.** Gallery of images of negatively stained thick filaments used in the reconstructions. All the filaments are oriented such that the bare zone would appear at the top of the image. In each case, a centrally located length about one-half of that shown was masked off for transforming, corresponding to  $8 \times 43.5$  nm repeats on the filament. Approximate magnification,  $94,000 \times$ .

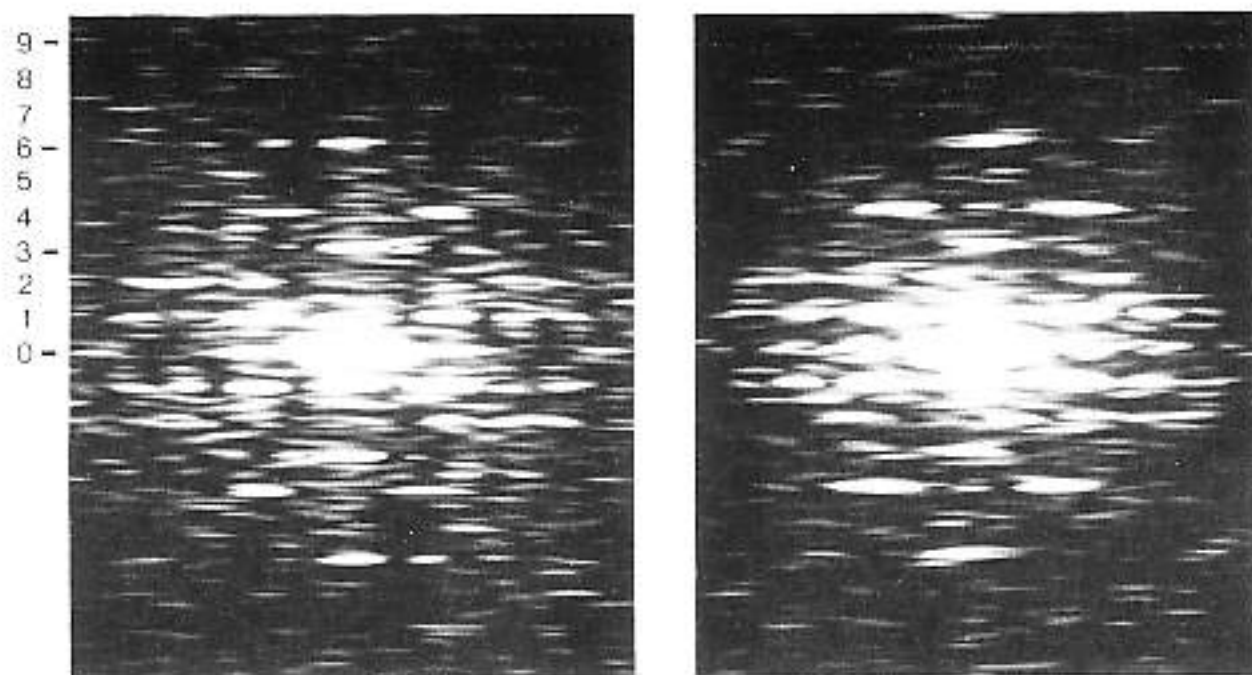


**Figure 3.** Computed transforms from the leftmost pair of filaments in Fig. 2. The patterns were photographed from the screen of an AED 767 raster graphics display. The numbering of the layer-lines, corresponding to a helical repeat of 43.5 nm, is indicated on the left. The intensities on the 1st and 4th and the meridional 3rd and 6th layer-lines are particularly strong.

layer-line ( $1/4.8 \text{ nm}^{-1}$ ) axially and to about  $1/5 \text{ nm}^{-1}$  radially, giving a uniform Fourier cut off. The data beyond  $1/7 \text{ nm}^{-1}$  are weak.

A contour map of the three-dimensional reconstruction is shown in Figure 6(a). The strongest feature, as expected, is the set of strong right-handed long-pitch helices seen in the shadowed preparation (Fig. 1(b)). This is demonstrated more clearly by the surface representation of the reconstruction shown in Figure 7(a). The inner core of the filament is strongly stain-excluding and shows essentially no detail out to a radius of about 8.5 nm. The helical ridges of crossbridges appear as if applied to this central

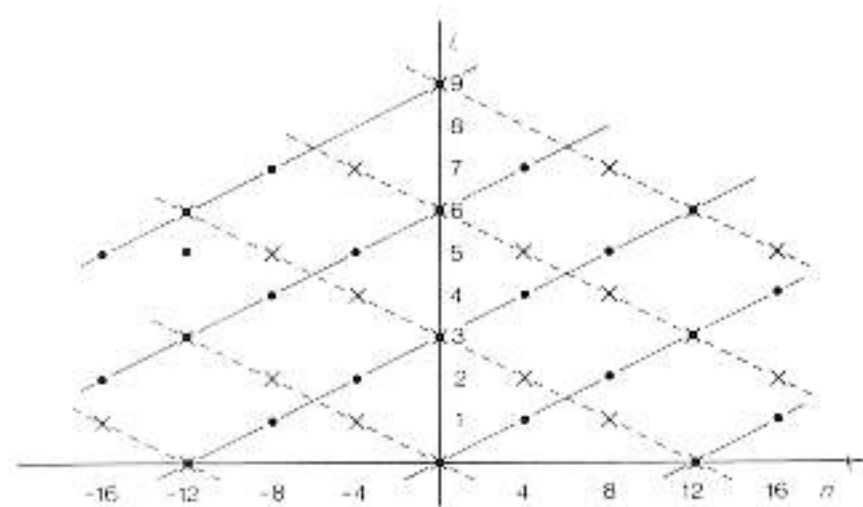


**Figure 4.** Indexing of the diffraction pattern for the tarantula thick filament, showing which orders ( $n$ ) of Bessel function occur on each layer-line ( $l$ ). The dots or crosses indicate that a particular peak in the diffraction pattern can be considered as arising from one or other side of the helix. Each basic helix has 12 units/turn and the structure is made from 4 such helices arranged with fourfold symmetry (Levine *et al.*, 1983). Such symmetry means that different orders of Bessel function (e.g. 4 and -8) begin to overlap even at low resolution and their contributions must be separated by combining data from different views before a reconstruction can be made.

core. The crossbridges extend to an outermost radius of about 16 nm, though this is difficult to judge precisely with negative staining.

The long-pitch helices have a zig-zag appearance (Fig. 6(a), and Fig. 7(a)), arising from strong ridges of density (denoted by R in Fig. 6(a)) at each 14.5 nm level. It is these ridges that give rise to the strong meridional intensities on the third and sixth layer-lines (Fig. 3). The nature of these morphological features is revealed more clearly by computing a reconstruction with the equatorial ( $l = 0$ ) data omitted, thus removing the central core of density from the filament (Fig. 6(b)). It can also be seen by superimposing the top few sections from the map in Figure 6(a), as shown in Figure 8(b). Viewed in this way it can be seen that the strong ridges of density arise from the superposition of a series of bi-lobal features, as indicated by the heavy boundaries drawn on the map in Figure 8(a). The equivalent features are also delineated on the surface map in Figure 7(b). We should like to suggest that each bi-lobal feature represents the two S1† heads of a myosin molecule.

The putative S1 heads of one myosin molecule have been labelled A1 and A2 in Figure 8(b), while the putative heads of the axially neighbouring molecule have been labelled B1 and B2. The two large lobes appear to connect onto the backbone through a smaller common domain, labelled A3 and B3. The two lobes (1 and 2) plus the smaller domain (3) together constitute the repeating morphological unit (crossbridge) on the outside of the filament. The strong ridges of density every 14.5 nm are thus produced by the stacking of one S1 head of one molecule (e.g. A2 in Fig. 8(b)) on the S1 head of an axially neighbouring molecule (e.g. B1 in Fig. 8(b)).

† Abbreviation used: S1, subfragment 1.

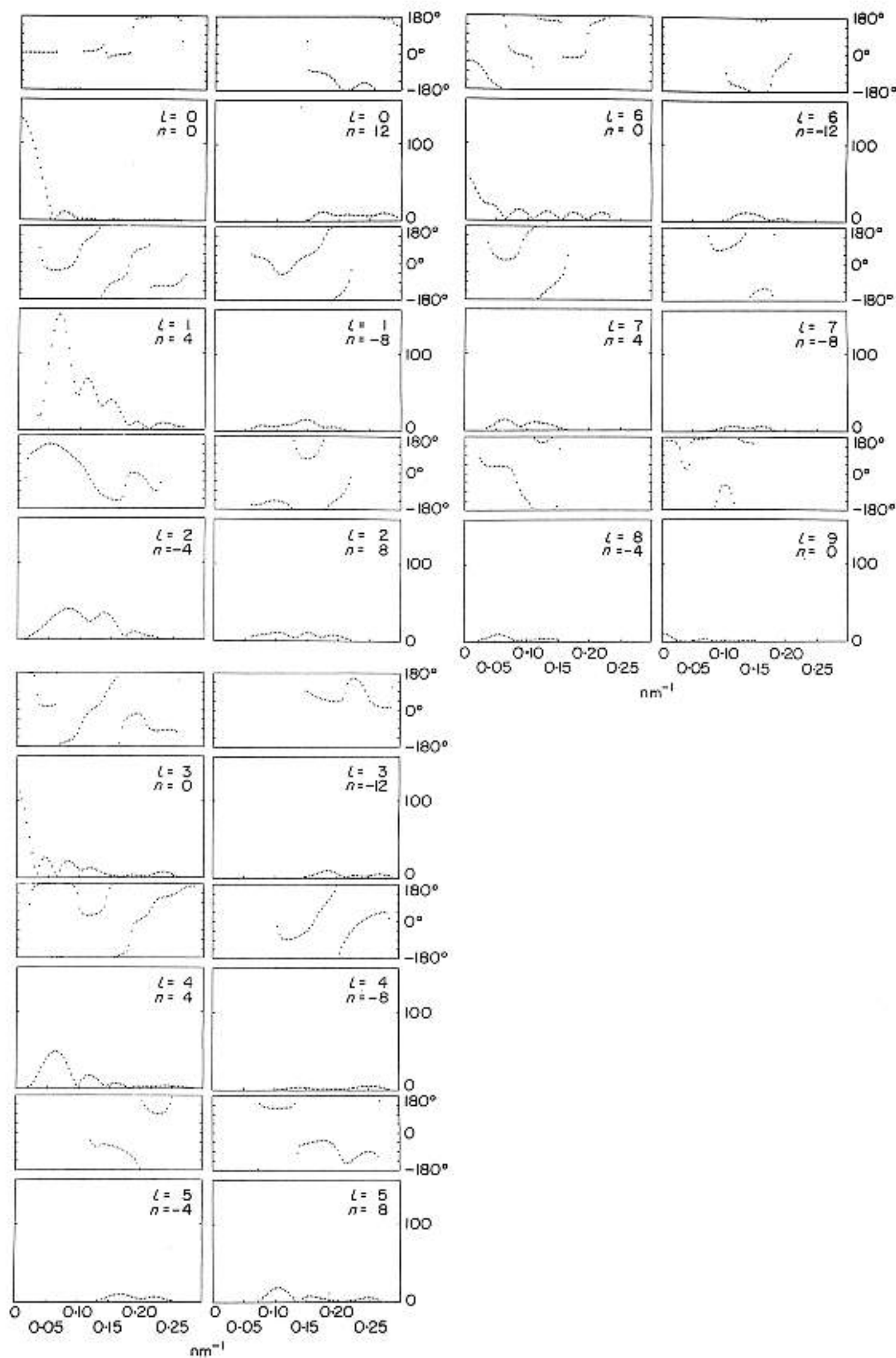


**Figure 5.** Separated Bessel function contributions on each layer-line, showing their amplitudes (lower part of each panel) and phases (upper part of each panel). These were calculated from the combined data from the particles shown in Fig. 2. The amplitude of the  $l = 0, n = 0$  term is plotted at one-tenth the scale of the others.

**Table 1**  
Summary of data on fitting particles†

Particle number	View angle (deg.)	Phase residual	Least-squares residual
761-1	6.5	53	0.34
758-1	17	50	0.31
826-1	0	—	0.24
811-2	15	50	0.29
793-1	21	50	0.37
811-1	7	38	0.37
758-3	9	51	0.29
769-1	27.5	49	0.33

† Particles are listed in the order shown from left to right in Fig. 2.

Angular orientation of particle relative to the average of the near and far sides of 826-1 as reference.

Weighted phase residual  $(\sum |F| \Delta \Theta^2 / \sum |F|)^{1/2}$  in degrees at the optimal position for fitting each particle against the averaged data from 826-1 as reference. Data close to the meridian on layer-lines  $l = 1$  to  $l = 9$  are included.

Least-squares residuals  $\sum |F_{\text{obs}} - F_{\text{calc}}|^2 / \sum |F_{\text{obs}}|^2$  from the Bessel separating program, corresponding to the lack of fit in solving eqn (1) in Materials and Methods, section (c). All data from layer lines  $l = 1$  to  $l = 9$  included, but  $l = 0$  excluded as its strength would dominate the weighting.

The change in directionality of the major connectivity in the density is seen clearly between A2 and B1, where the plane of sectioning is

particularly favourable. This division of density, if correct, produces a feature containing two equally sized domains springing from a common region on the backbone, which looks very like the images of individual myosin molecules seen in shadowed preparations (Elliott & Offer, 1978) or in negatively stained filaments with extended heads (Knight & Trinick, 1984).

An alternative interpretation that we considered, but discounted, was to ascribe the features labelled B1, A2 and B3 (Fig. 8(b)) to a single myosin crossbridge, which would join the backbone at the point indicated by the B3 arrowhead. This interpretation would lead to considering half of B1 plus A2 as one S1 head and half of B1 plus B3 as the other. However, this division is much less symmetrical than the bi-lobal one described above, as regards both density and shape, and does not produce an overall shape resembling the heads seen in isolated molecules. We therefore prefer the bi-lobal division of density described above and illustrated in Figures 7(b) and 8(a).

Each elongated domain ascribed to a myosin head is curved and is at least 15 nm long, though it is not clear where the domains terminate as they join onto the backbone of the filament. The domains are about 5 nm wide and 3 to 4 nm deep in the aspect presented by A2 or B1 in Figure 8(b).

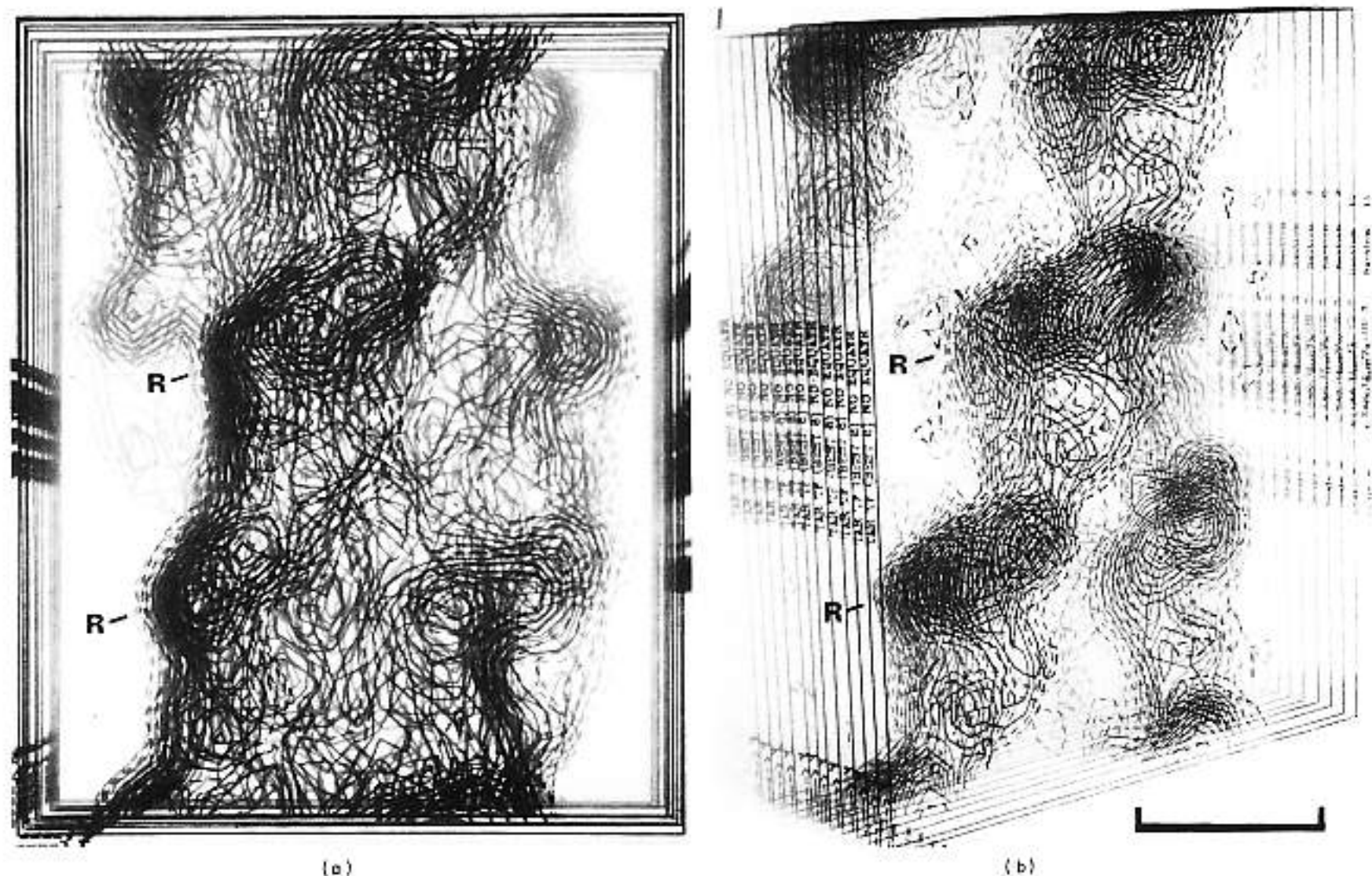


**Figure 6.** Contour maps of reconstructions from the data shown in Fig. 5. (a) Including the equatorial ( $l = 0$ ) data. (b) Excluding the equatorial ( $l = 0$ ) data. The maps are contoured on sections parallel to the axis of the filament, which runs vertically in the diagram. Only the half filament nearer the viewer is plotted and a length of 43.5 nm corresponding to one helical repeat is shown. The strong ridges at each 14.5 nm level are denoted by R (see the text). The bare zone of the thick filament would be at the top in this diagram. The contours represent exclusion of stain. The scale bar represents 10 nm.

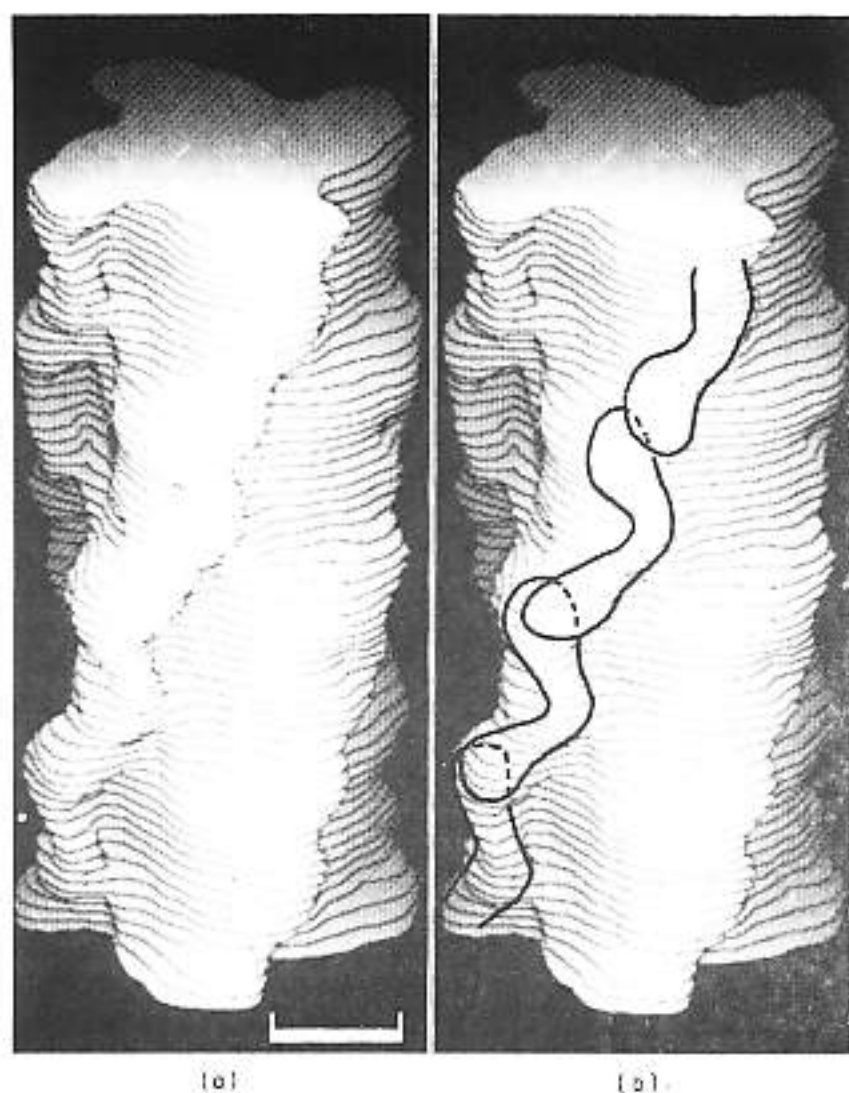


**Figure 7.** (a) Surface representation of the thick filament reconstruction (plotted using a computer program written by E. H. Egelman). The contour level was chosen so that the plotted surface represents the position of maximum density gradient in the map and thus the likely boundary between stain and protein. The right-handed long-pitch helices are the strongest surface feature and their zig-zag nature is apparent. The separation between plotted sections is 1 nm, a length of 60 nm is shown and the bare zone would be at the top. (b) As (a) but with the putative arrangement of myosin heads superimposed (see the text and also Fig. 8). The scale bar represents 10 nm.

This would give a volume in the range 120 to 160 nm<sup>3</sup>, if the domain were ellipsoidal, where the uncertainty arises from the difficulty of estimating precise dimensions in negative staining. In the filament, head number 1 points towards the bare zone, making a slew angle of about 8° with the filament axis, while head number 2 points away from the bare zone making a slew angle of about 45° with the filament axis (Fig. 8(b)). The angle between the heads is about 127°. The dimer nature of the myosin molecule implies that a twofold axis of symmetry might be expected. Here an approximate local twofold axis relates the two domains forming one of the bi-lobal features, making a slew angle of about 72° with the filament axis and lying in a plane about 10 nm from the axis. The division of density described means that although the shapes of the two lobes 1 and 2 are

very similar, their environments are rather different, with lobe 1 close to the backbone and somewhat buried whereas lobe 2 is much more exposed.

#### 4. Discussion

In this study, we have used improved structural techniques to observe features of the crossbridges of a thick filament that have not been seen in previous thick filament reconstructions (cf. Stewart *et al.*, 1981; Vibert & Craig, 1983).

For several reasons we believe that the filaments we have observed by negative staining have a structure similar to that occurring in intact, relaxed tarantula muscle. (1) The filaments were maintained under relaxing conditions until the instant of staining; this represents an improvement over previous studies, where the filaments were rinsed with a simple ammonium acetate solution prior to staining, which may have produced some (unknown) degree of rigor (Kensler & Levine, 1982a; Vibert & Craig, 1983). (2) We have shown that the filaments as isolated have non-phosphorylated regulatory light chains (Craig *et al.*, 1985). Thus, by comparison with the closely related *Limulus* muscle, which is activated by light chain phosphorylation (cf. Sellers, 1981), our filaments are in the inactive (relaxed) state. (3) The filaments were observed over holes in the carbon support film, thus eliminating any interaction of the crossbridges with the substrate, which can induce a disordering of the crossbridge array (cf. Trinick & Elliott, 1979). (4) Micrographs were taken with minimal electron dose to minimize changes in surface features that occur as a result of stain migration under high electron doses (Unwin, 1974). (5) Diffraction patterns of the filament images are similar to the myosin portions of X-ray diffraction patterns of relaxed whole tarantula muscle (Wray, 1982, and personal communication).

Computer programs were developed for this study that allowed an improvement in the resolution of the three-dimensional reconstruction compared with earlier work on the closely related *Limulus* muscle (Stewart *et al.*, 1981), where each crossbridge appeared as a single morphological unit. With low, even-order helical symmetry, Bessel functions of different orders start to overlap at fairly low resolution on any given layer-line, limiting the resolution of the three-dimensional map obtainable from a single view. By separating the Bessel functions computationally (see Materials and Methods), a higher resolution has been obtained showing the repeating morphological unit as three domains. The two large domains (1 and 2 in Fig. 8(b)) are of similar size and shape and are most easily interpreted as the two heads of a single myosin molecule, while the third domain (3 in Fig. 8(b)) may represent part of the S2 region or the

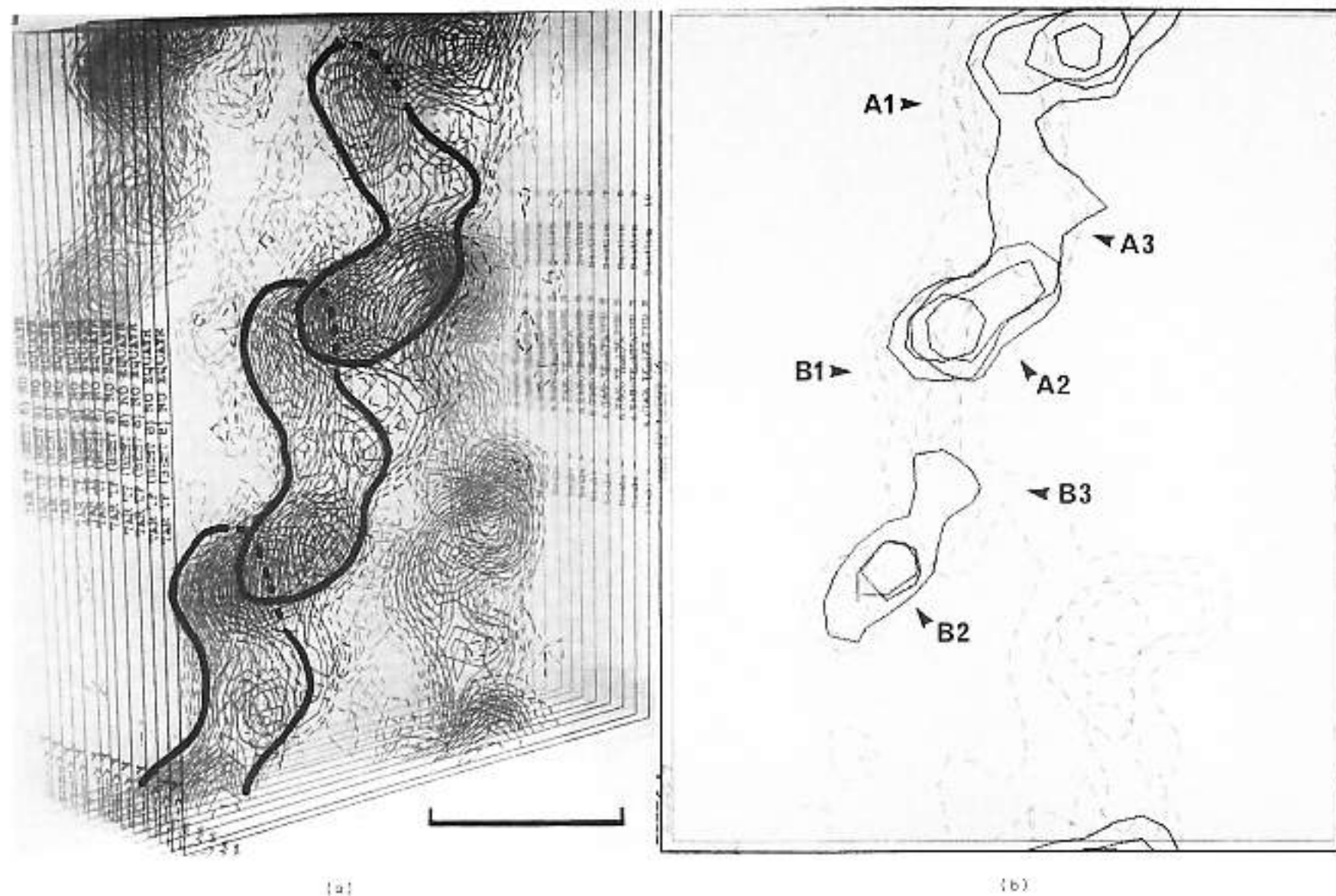


**Figure 8.** (a) Contour map of the reconstruction of the thick filament using the data in Fig. 5 but with the equator ( $l = 0$ ) omitted (as Fig. 6(b)). The superimposed heavy boundaries indicate the bilobed features, thought to represent the 2 S1 heads of a single myosin molecule (see the text). The 2 putative heads of one molecule stack, respectively, under and over the heads of the axially neighbouring molecules. (b) Superposition of 4 neighbouring sections from the map shown in Fig. 6(a), spanning a depth of 5.8 nm. The outermost pair of sections are shown as unbroken contours and the next pair as broken contours. A1 and A2 represent the putative heads of one myosin molecule, while B1 and B2 represent the heads of the next axially positioned molecule. The large domains appear to connect to the backbone through a smaller common domain (A3, B3). The shape and connectivity of the density features can thus be seen, as can the abrupt change in direction of features between A2 and B1. The zig-zag arrangement of density features forming the long-pitch helices is also clear. The bare zone would be at the top of the diagram. The scale represents 10 nm.

unresolved, narrow necks of the two heads. This is the first time that the spatial arrangement of the two heads of the myosin molecule on a relaxed thick filament has been resolved. Use of these Bessel separation programs on *Limulus* filaments (Stewart *et al.*, 1985) has now shown finer substructure within that which was seen previously as a single domain crossbridge (Stewart *et al.*, 1981). In the case of scallop, which has higher-order  $N = 7$  rotational symmetry (Vibert & Craig, 1983), there is no problem with overlap of Bessel functions, but the resolution in this case appears to be limited by an inherently less stable crossbridge array in these filaments.

Our interpretation of the reconstructed map is that one of the two elongated heads of a myosin molecule points approximately axially towards the bare zone, while the other points in the opposite direction making a slew angle of about  $45^\circ$  with the axis (see Fig. 8). Thus, each head of a given molecule stacks, respectively, under or over one of

the heads of the two axially neighbouring molecules. The under and over packing of heads produces the continuity of the strong right-handed long-pitch helices. This interpretation of the map in terms of the two heads of a molecule produces an envelope that closely resembles the head structure seen in shadowed pictures of isolated myosin molecules (Elliott & Offer, 1978). Each head has a similar curved shape consistent with previous reconstructions of S1-decorated thin filaments (Moore *et al.*, 1970; Taylor & Amos, 1981) and with details seen in isolated thick filaments (Knight & Trinick, 1984). The volume of each head is about  $140 \text{ nm}^3$ , which agrees reasonably well with that estimated from isolated heads (Taylor & Amos, 1981), from heads on isolated molecules (Elliott & Offer, 1978), and from the estimated molecular weight of 130,000 for the head (Margossian *et al.*, 1981), particularly as it is unclear how much of the head is included within our quoted dimensions. While our interpretation of the density in terms of

the two heads is not the only one possible, it is the most consistent with the two-headed nature of the myosin molecule and with the myosin head shape, volume and size determined by other techniques. With this (or with any other plausible) interpretation, the long axis of the head must run close to the filament backbone as was also found for the scallop (Vibert & Craig, 1983). X-ray diffraction studies (Wray *et al.*, 1975; Haselgrove, 1980), which suggest that the myosin heads in relaxed muscles generally tilt considerably away from the perpendicular to the filament axis, are consistent with this finding.

The structure we have described has implications for contraction mechanisms. The stacking interaction between heads from axially neighbouring myosin molecules suggested by our interpretation is very striking. It seems that in the relaxed state, with dephosphorylated regulatory light chains, the crossbridges are closely associated with the thick filament backbone and with each other. It is possible that this ordered structure is thus physically "locked" (like a zip fastener) through the tips of the heads, helping to maintain the "off" state of the filament, by preventing interaction with actin. The intermolecular interactions we observe may be related to the co-operative switching "on" of filaments that occurs when some muscles are activated (cf. Chantler *et al.*, 1981), allowing the heads to interact with actin. We are currently studying the structural changes that occur in these myosin filaments when they are activated by phosphorylation of the light chains (R. Craig & J. Kendrick-Jones, unpublished results).

The crossbridge arrangements in several thick filaments (*Limulus*, lobster, scallop and frog) have been investigated both by X-ray diffraction (Wray *et al.*, 1975; Haselgrove, 1980) and more recently and more directly by electron microscopy (Stewart *et al.*, 1981; Kensler & Levine, 1982*a,b*; Vibert & Craig, 1983; Kensler & Stewart, 1983). We have studied tarantula thick filaments (cf. also Levine *et al.*, 1983), since they appear to be amongst the most highly ordered of all thick filaments and thus can be considered as "model" structures, offering greater insights into crossbridge organization than do other species. A disposition of the myosin heads close to the backbone and pointing in opposite directions along the filament as found here for tarantula was also suggested (though less directly) by X-ray modelling studies of relaxed frog striated muscle (Haselgrove, 1980). This apparent similarity between two very different species of filament suggests that our conclusions concerning the positioning of the myosin heads may also be true in other less ordered filaments.

We thank Dr John Wray for discussion and for lending us an unpublished X-ray diffraction pattern of relaxed tarantula muscle, Drs H. E. Huxley and A. Klug for comments on the manuscript, Mr Claudio Villa for excellent assistance with photography, and Mrs J. M. Smith for help with computer programs. R. P. was the

recipient of the Vollmer Fellowship from the Instituto Venezolano de Investigaciones Científicas (IVIC), Venezuela, from 1980 to 1982, and R. C. held a Medical Research Council postdoctoral fellowship.

## References

- Amos, L. A. (1975). *Proceedings of the 33rd Annual Meeting of the Electron Microscopy Society of America* (Bailey, G. W., ed.), pp. 290-291, Claitor's Publishing Division, Baton Rouge.
- Amos, L. A. (1976). *Proceedings of the 6th European Congress on Electron Microscopy, Jerusalem* (Brandon, D. G., ed.), pp. 14-19, Tal International Publishing Co., Israel.
- Arndt, U. W., Barrington-Leigh, J., Mallett, J. F. W. & Twinn, K. E. (1969). *J. Phys. E. ser. 2*, **2**, 385-387.
- Chantler, P. D., Sellers, J. R. & Szent-Györgyi, A. G. (1981). *Biochemistry*, **20**, 210-216.
- Craig, R. & Padrón, R. (1982). *J. Muscle Res. Cell Motil.* **3**, 487.
- Craig, R., Padrón, R. & Kendrick-Jones, J. (1985). *Biophys. J.* **47**, 469a.
- Crowther, R. A., DeRosier, D. J. & Klug, A. (1970). *Proc. Roy. Soc. ser. A*, **317**, 319-340.
- Depue, R. H. & Rice, R. V. (1965). *J. Mol. Biol.* **12**, 302-303.
- DeRosier, D. J. & Klug, A. (1972). *J. Mol. Biol.* **65**, 469-488.
- DeRosier, D. J. & Moore, P. B. (1970). *J. Mol. Biol.* **52**, 355-369.
- Elliott, A. & Offer, G. (1978). *J. Mol. Biol.* **123**, 505-519.
- Haselgrove, J. C. (1980). *J. Muscle Res. Cell Motil.* **1**, 177-191.
- Huxley, H. E. (1957). *J. Biophys. Biochem. Cytol.* **3**, 631-648.
- Huxley, H. E. (1963). *J. Mol. Biol.* **7**, 281-308.
- Huxley, H. E. (1969). *Science*, **164**, 1356-1366.
- Huxley, H. E. & Brown W. (1967). *J. Mol. Biol.* **30**, 383-434.
- Kensler, R. W. & Levine R. J. C. (1982*a*). *J. Cell Biol.* **92**, 443-451.
- Kensler, R. W. & Levine R. J. C. (1982*b*). *J. Muscle Res. Cell Motil.* **3**, 349-361.
- Kensler, R. W. & Stewart, M. (1983). *J. Cell Biol.* **96**, 1797-1802.
- Knight, P. & Trinick, J. (1984). *J. Mol. Biol.* **177**, 461-482.
- Levine, R. J. C., Kensler, R. W., Reedy, M. C., Hofmann, W. & King, H. A. (1983). *J. Cell Biol.* **97**, 186-195.
- Margossian, S. S., Stafford, W. F. & Lowey, S. (1981). *Biochemistry*, **20**, 2151-2155.
- Moore, P. B., Huxley, H. E. & DeRosier, D. J. (1970). *J. Mol. Biol.* **50**, 279-295.
- Padrón, R. & Huxley, H. E. (1984). *J. Muscle Res. Cell Motil.* **5**, 613-655.
- Padrón, R., Crowther, R. A. & Craig, R. (1984). *Biophys. J.* **45**, 10a.
- Sellers, J. R. (1981). *J. Biol. Chem.* **256**, 9274-9278.
- Stewart, M., Kensler, R. W. & Levine, R. J. C. (1981). *J. Mol. Biol.* **153**, 781-790.
- Stewart, M., Kensler, R. W. & Levine, R. J. C. (1985). *J. Cell Biol.* In the press.
- Taylor, K. A. & Amos, L. A. (1981). *J. Mol. Biol.* **147**, 297-324.
- Trinick, J. & Elliott, A. (1979). *J. Mol. Biol.* **131**, 133-136.

Unwin, P. N. T. (1974). *J. Mol. Biol.* **87**, 657-670.

Unwin, P. N. T. & Henderson, R. (1975). *J. Mol. Biol.* **94**, 425-440.

Vibert, P. & Craig, R. (1982). *J. Mol. Biol.* **157**, 299-319.

Vibert, P. & Craig, R. (1983). *J. Mol. Biol.* **165**, 303-320.

Williams, R. C. & Fisher, H. W. (1970). *J. Mol. Biol.* **52**, 121-123.

Wray, J. S. (1979). *Nature (London)*, **277**, 37-40.

Wray, J. S. (1982). In *Basic Biology of Muscles: A Comparative Approach* (Twarog, B. M., Levine, R. J. C. & Dewey, M. M., eds), pp. 29-36, Raven Press, New York.

Wray, J. S., Vibert, P. J. & Cohen, C. (1975). *Nature (London)*, **257**, 561-564.

*Edited by M. F. Moody*